Interaction between Theory and Practice in Civil Engineering and Construction
Edited by Komurlu, R., Gurgun, A. P., Singh, A., and Yazdani, S.

ISBN: 978-0-9960437-2-4

DEFLECTION PREDICTION OF TWO-SPAN CONTINUOUS CONCRETE BEAMS REINFORCED WITH GFRP BARS

KARAM MAHMOUD and EHAB EL-SALAKAWY

Dept of Civil Engineering, University of Manitoba, Winnipeg, Manitoba, Canada

Continuous beams are main structural members in many reinforced concrete (RC) applications such as parking garages and bridges, which are vulnerable to harsh environments. The use of glass fiber-reinforced polymers (GFRP) bars in such structures has proven to be a good solution to overcome the steel corrosion problem. In GFRP-RC beams, deflection is a concern and may govern the design; thus, attempts have been made to propose models to predict the effective moment of inertia and consequently the deflection. The current prediction models were verified against deflection of simply-supported beams. In this paper, available predictions models are compared to the experimental deflections of two-span continuous beams. Eight rectangular beams (200×300 mm) continuous over two equal spans of 2,800 mm each were constructed and tested to failure. All beams were reinforced with GFRP bars and stirrups. The test variables included concrete strength, longitudinal reinforcement ratio and transverse reinforcement ratio. The comparison revealed that the investigated models reasonably predicted the deflection at service load level while they underestimated the deflection at higher load levels. These models require to be modified in order to yield better predictions of the deflection at lower and higher load levels than service load.

Keywords: Effective moment of inertia, High strength concrete, Fiber reinforced polymer, Modulus of elasticity, Cracking moment, Service moment.

1 INTRODUCTION

Fiber reinforced polymer (FRP) bars are a viable alternative to conventional steel reinforcement in structures, which are exposed to aggressive environment because of their superior corrosion resistance. However, the low modulus of elasticity of the FRP bars, compared to that of steel bars, results in much lower post-cracking flexural stiffness and consequently large deflections. This raised concerns about the performance of FRP-reinforced concrete (RC) members especially at service load. Extensive studies investigated the applicability of deflection prediction models used for steel-RC beams to FRP-RC beams and proposed modified versions of these models to reasonably predict the deflection behavior of such beams (Mota *et al.* 2006, Bischoff 2005, Bischoff and Gross 2011). However, all these studies focused on FRP-RC simply-supported beams and one-way slabs and no attention was given to continuous beams, which are main structural elements commonly used in structural applications. In this paper, the load-deflection behavior of eight two-span continuous concrete beams

reinforced with GFRP bars is compared to the predictions of models available in the literature.

2 REVIEW OF MODELS FOR EFFECTIVE MOMENT OF INERTIA

In this paper, four models available in the literature are reviewed in this section (Table 1). These models were verified previously against results of simple beams with rectangular sections. The first model is adopted by ISIS design manual 3 (2007). This model was previously evaluated by Mota *et al.* (2006) and it was found that it gives consistently conservative results for simply-supported beams.

The second model is a modified version of Branson's expression recommended by the ACI 440.1R-06. The modification factor ($\beta_d = 0.2(\rho/\rho_b)$) accounts for the reduced tension stiffening in FRP-RC members. In the ACI 440.1R (2015), another expression for the effective moment of inertia is introduced which is based on a model proposed by Bischoff (2005). Also, a modification factor ($\gamma = 1.72\text{-}0.72\ (M_{cr}/M_a)$) is added to the equation to account for the variation of the stiffness along the member length where M_{cr} is the cracking moment and M_a is the moment at which deflection is to be calculated.

Bischoff and Gross (2011) introduced an equivalent moment of inertia based on integration of curvature to account for changes in member stiffness along the span. Closed-form solutions of integrated expressions for deflection are expressed in terms of an equivalent moment of inertia.

Table 1. Review of effective moment of inertia equations.

Reference	Effective moment of inertia	Related formulas
ISIS Design M3 (2007)	$I_e = I_t I_{cr} / \left(I_{cr} + \left(1 - 0.5 \left(M_{cr} / M_a \right)^2 \right) \left(I_t - I_{cr} \right) \right)$	$I_{cr} = \frac{bd^3}{3} k^3 + n_f A_f d^2 (1 - k^2)$
ACI 440.1R-06	$I_e = \left(M_{cr} / M_a \right) \beta_d I_g + \left[1 - \left(M_{cr} / M_a \right)^3 \right] I_{cr} \le I_g$	$k = \sqrt{2\rho_f n_f + (\rho_f n_f)^2} - \rho_f n_f$
ACI 440.1R-15	$I_e = I_{cr} / \left(1 - \gamma \left(M_{cr} / M_a \right)^2 \left[1 - I_{cr} / I_g \right] \right) \le I_g$ where $M_a \ge M_{cr}$	$n_f = \frac{E_f}{E_c}$
Bischoff and Gross (2011)	$I_e^{'} = I_{cr} / \left[1 - \gamma \eta \left(M_{cr} / M_a \right)^2 \right] \le I_g$ where $\eta = 1 - \left(I_{cr} / I_g \right), \gamma = 1.7 - 0.7 \left(\frac{M_{cr}}{M_a} \right)$	$M_{cr} = \frac{0.62 \lambda \sqrt{f_c^{'}} I_g}{y_t}$ $I_g = \frac{bh^3}{12}$

M_{cr}=cracking moment; M_a=applied moment; I_g=I_t=gross moment of inertia; I_{cr} =moment of inertia of transformed cracked section; k=ratio of the neutral axis depth to reinforcement depth; E_c=modulus of elasticity of concrete; E_f = modulus of elasticity of reinforcement; b= width of the beam; h=overall height of the beam; d= effective depth of the beam; ρ_f = reinforcement ratio; $f_c^{'}$ = concrete strength; A_f = reinforcement area; y_t = distance from cantorial axis of gross section to tension face; λ= factor accounts for concrete density.

3 EXPERIMENTAL INVESTIGATION

Eight large-scale RC continuous beams were constructed and tested to failure. All test beams had a rectangular cross (200×300 mm) and were continuously supported over

two equal spans of 2,800 mm each. All beams were reinforced with GFRP bars and stirrups. The longitudinal reinforcement ratio was 0.8% in two beams, while it was 1.2% in the other six beams. The shear reinforcement ranged from half to twice the minimum shear reinforcement as specified by the Canadian standards CSA/S806-12 (CSA 2012). Dimensions and details of the test specimens are shown in Figure 1.

The beams were tested under a two-point loading system in each span. The strains in the concrete, longitudinal reinforcement, and stirrups were measured at critical locations using electrical strain gauges. The deflection was measured using linear variable differential transducers (LVDTs) at mid-span, and at each loading point. Moreover, two load cells were used to measure the reactions at the exterior supports.

The specimen designation can be explained as follows: The first letter indicates the concrete strength ("N" for normal strength and "H" for high strength). The second number indicates the percentage of the longitudinal reinforcement ratio (0.8% and 1.2%). The third number indicates the amount of transverse reinforcement ("1.0" for minimum and "0.5" and "2.0" for half and twice the minimum, respectively).

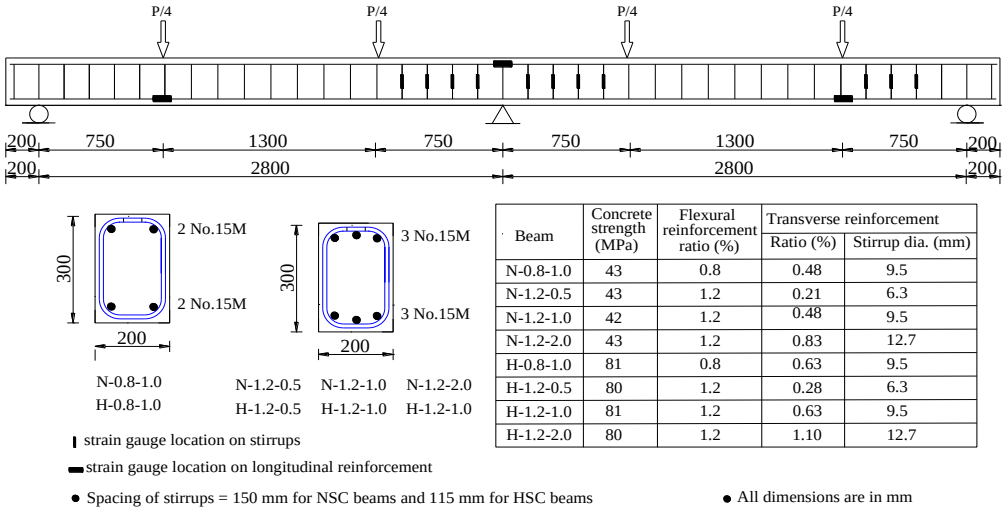

Beam	Concrete strength (MPa)	Flexural reinforcement ratio (%)	Transverse reinforcement	
			Ratio (%)	Stirrup dia. (mm)
N-0.8-1.0	43	0.8	0.48	9.5
N-1.2-0.5	43	1.2	0.21	6.3
N-1.2-1.0	42	1.2	0.48	9.5
N-1.2-2.0	43	1.2	0.83	12.7
H-0.8-1.0	81	0.8	0.63	9.5
H-1.2-0.5	80	1.2	0.28	6.3
H-1.2-1.0	81	1.2	0.63	9.5
H-1.2-2.0	80	1.2	1.10	12.7

Figure 1. Details of test beams.

The properties of the used sand-coated GFRP bars are reported in Table 2. All beams were constructed using normal weight concrete. The average concrete strength obtained on the test day ($f_c^{'}$) is reported in Figure 1.

Table 2. Properties of the reinforcing bars and stirrups.

Bar type	Diameter (mm)	Area (mm^2)	f_{fu} (MPa)	E_f (GPa)	ε_{fu} (%)
Straight bar	15.9	198	1442	67	2.1
Stirrups	6.3	32	1383	53	2.6
	9.5	72	1195	45	2.7
	12.7	127	1328	53	2.5

f_{fu} = tensile strength of the bar; ε_{fu} = rupture strain of the bar.

4 TEST RESULTS

Test results and detailed discussion of cracking behavior, deflection, strains in longitudinal reinforcement and concrete, moment redistribution and shear capacity of the test beams can be found elsewhere (Mahmoud and El-Salakawy 2014, 2016). In this paper, the discussion focuses on the deflection behavior and the comparison between experimental and predicted deflections.

4.1 Load-deflection Response

The load-deflection relationship at midspan for all test beams is shown in Figure 2. The typical load-deflection graph can be defined by two distinct stages; pre-cracking, characterized by small deflection, and post-cracking, in which significant deflection was observed. In the post-cracking stage, the flexural stiffness of the beam was mainly dependent on the axial stiffness of the reinforcing bars. Therefore, at the same load level, the measured deflection in beams with 0.8% longitudinal reinforcement ratio was higher than that in beams with 1.2%. Also, beams made of high strength concrete (HSC) had higher flexural stiffness; therefore, the deflection graphs for HSC beams were steeper than those of the normal strength concrete (NSC) ones.

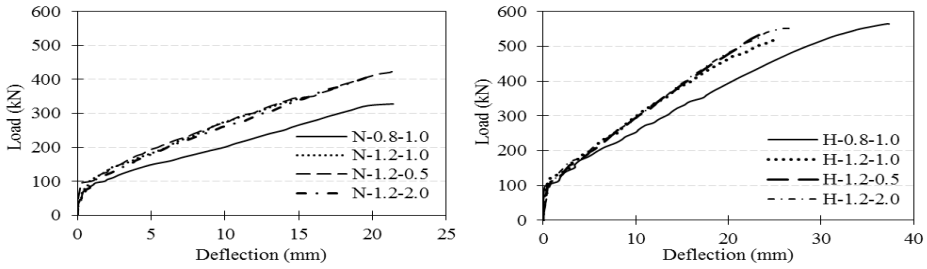

Figure 2. Load versus mid-span deflection of test beams.

5 COMPARISON OF EXPERIMENTAL AND PREDICTED DEFLECTION

Figure 3 shows the experimental and predicted load-deflection relationships for representative beams with different longitudinal and transverse reinforcement ratios and concrete strength. It can be seen that all investigated models reasonably predicted the mid-span deflection up to approximately 50% of the ultimate load; however, they highly underestimated the deflection at higher load levels. The difference between the experimental and predicted deflections increased in beams with lower reinforcement ratio (0.8%) as well as for HSC beams compared to those with 1.2% reinforcement ratio and NSC, respectively. For all test beams, the predicted deflections were close to the experimental ones near the service load level; however, the slope of the post-cracking stage is shallower than that predicted by all the evaluated models of effective moment of inertia. Also, these models yielded poor predictions of the deflection at load levels less than service load. Most structures encounter higher loads than service load before reaching failure. In case of steel-RC members the deflections do not increase significantly because of the high modulus of elasticity of the steel bars; however, FRP-RC members exhibit large deflections with a slight increase in the load beyond their

service load (Figure 3). This large deflection may cause damage to other elements attached to such members. Thus, it is required to modify these models to reasonably predict the deflection behavior for the full range of loading not only at service load.

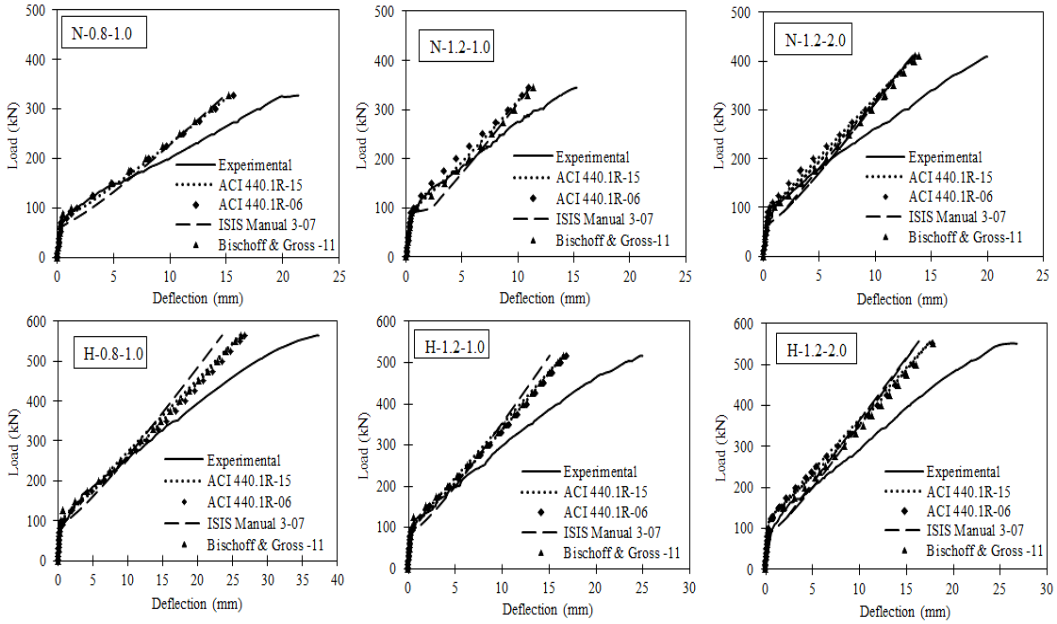

Figure 3. Load-deflection relationship for representative beams.

Table 3. Statistical comparison of experimental-to-predicted deflection.

Reference	@Cracking load		@1.2 P_{cr}		@Service load		@0.8 P_u	
	Mean	COV	Mean	COV	Mean	COV	Mean	COV
ACI 440.1R-15	2.59	0.33	1.42	0.24	1.17	0.13	1.32	0.04
ACI 440.1R-06	1.51	0.31	1.61	0.12	1.36	0.08	1.31	0.04
ISIS Manual 3 (2007)	0.51	0.29	0.67	0.24	0.94	0.17	1.33	0.06
Bischoff & Gross (2011)	1.65	0.28	1.12	0.23	1.05	0.12	1.26	0.04

Also, a statistical comparison of the experimental and predicted deflection considering the results of all tested beams at different load levels is presented in Table 3. The load levels considered herein are the cracking load (P_{cr}), 1.2 P_{cr}, service load taken as 43% of the ultimate load (Mousavi and Esfahani 2012), and at 80% of the ultimate load. It can be seen that the models proposed by ACI 440.1R (2006 and 2015) and Bischoff and Gross (2011) underestimated the deflection at P_{cr} and 1.2 P_{cr} while better predictions were obtained at the service load level. Also, the newly adopted model by ACI 440.1R -15 yielded better predictions compared to that of the ACI 440.1R-06, especially at the service load level. On the other hand, the model adopted by ISIS design manual 3 (2007) overestimated the measured deflection; highly at P_{cr} and 1.2 P_{cr} and slightly at the service load level. With further increase in the load

beyond the service load level, all models underestimated the deflection where the average experimental-to-predicted deflection ratio ranged from 1.26 to 1.33.

6 CONCLUSIONS

Based on the comparison between the experimental and predicted deflection by different models available in literature, the following conclusions can be drawn.

1) All evaluated models fairly predicted the mid-span deflection of GFRP-RC continuous beams up to the service load level. Also, these models underestimated the deflection of beams with low reinforcement ratios and HSC beams at high levels of loading.

2) At service load level, both models proposed by Bischoff and Gross (2011) and ISIS design manual 3 (2007) yielded the best predictions with a mean experimental-to-predicted deflection ratio of 1.05 and 0.94, respectively. The models proposed by ACI 440.1R (2006 and 2015) underestimated the deflection where the mean experimental-to-predicted deflection ratio was 1.36 and 1.17, respectively.

Acknowledgments

The financial support received from the Natural Science and Engineering Research Council of Canada, through the Canada Research Chairs program is sincerely appreciated as well as the help received from the technical staff of Structural Laboratory at the University of Manitoba.

References

ACI (American Concrete Institute), Guide for the design and construction of structural concrete reinforced with FRP bars, *ACI 440.1R-06*, Farmington Hills, MI, 2006.

ACI (American Concrete Institute), Guide for the design and construction of structural concrete reinforced with FRP bars, *ACI 440.1R-06*, Farmington Hills, MI, 215.

Bischoff, P., Reevaluation of deflection prediction for concrete beams reinforced with steel and fiber reinforced polymer bars, *Journal of Structural Engineering*, 131(5), 752-767, 2005.

Bischoff, P. and Gross, S, Equivalent moment of inertia based on integration of curvature, *Journal of Composites for Construction*, 15(3), 263-273, June, 2011.

CSA (Canadian Standard Association), Design and construction of building structures with fibre-reinforced polymers, *S806-12*, Rexdale, ON, Canada, 2012.

ISIS Canada Corporation, Reinforcing concrete structures with fiber reinforced polymers, *ISIS Canada: Design Manual No.3*, The Canadian Network of Centers of Excellence on Intelligent Sensing for Innovative Structures, Winnipeg, Manitoba, Canada, 2007.

Mahmoud, K., and El-Salakawy, E., Shear strength of GFRP-reinforced concrete continuous beams with minimum transverse reinforcement, *Journal of Composites for Construction*, ASCE, 18(1), 04013018, Feb., 2014.

Mahmoud, K., and El-Salakawy, E., Effect of transverse reinforcement ratio on the shear strength of GFRP-RC continuous beams, *Journal of Composites for Constructio*n, 20(1), 04015023, Feb., 2016.

Mota, C., Alminar, S., and Svecova, D., Critical review of deflection formulas for FRP-RC members, *Journal of Composites for Constructio*n, 10(3), 183-194, June, 2006.

Mousavi, S. and Esfahani, M. Effective moment of inertia prediction of FRP-reinforced concrete beams based on experimental results, *Journal of Composites for Construction*, 16(5), 490-498, October, 2012.